Strongly correlated regimes in a double quantum-dot device

P. S. Cornaglia and D. R. Grempel

CEA-Saclay, DSM/DRECAM/SPCSI, Bât. 462, F-91191 Gif-sur-Yvette, France

The transport properties of a double quantum-dot device with one of the dots coupled to perfect conductors are analyzed using the numerical renormalization group technique and slave-boson mean-field theory. The coupling between the dots strongly influences the transport through the system leading to a non-monotonic dependence of the conductance as a function of the temperature and the magnetic field. For small inter-dot coupling and parameters such that both dots are in the Kondo regime, there is a two-stage screening of the dot's magnetic moments that is reflected in the conductance. In an intermediate temperature regime Kondo correlations develop on one of the dots and the conductance is enhanced. At low temperatures the Kondo effect takes place on the second dot leading to a singlet ground state in which the conductance is strongly suppressed.

Since the prediction[1,2] of the occurrence of the Kondo effect in a single quantum dot (QD) device and its subsequent experimental observation[3], several single and double quantum dot devices (DQDD) have been studied both theoretically[4,5] and experimentally.[6,7] The interest in this systems stems form their potential applications to quantum and classical computing[8,9] and their usefulness as model systems for the study of the physics of strongly correlated electrons.[6]

In its simplest form, the Kondo effect consists in the screening of a localized spin 1/2 magnetic moment anti-ferromagnetically coupled to a conduction-electron band and appeared originally in the context of magnetic impurities in a metallic host. In a QD device Coulomb repulsion and spatial confinement result in charge quantization and its transport properties are dominated by the Coulomb blockade. When the charge on the QD is close to an odd integer the Kondo efect takes place and it results in perfect transmission through the system at sufficiently low temperatures in a wide range of gate voltages.

When two dots are coupled, a richer and more complicated behavior may arise[4,6,10] including the possibility of observing quantum phase transitions.[11]

In this paper we present a detailed study of a DQDD in which only one of the dots is coupled to the leads (see Figure 1). We discuss the case in which the QDs are very small and have a single relevant energy level at energies ε_a and ε_b and large charging energies U_a and U_b, where the indices a and b denote the two dots. The position of energy levels of the dots and the strength of the coupling between them t_{ab} can be tuned by applying gate voltages in semiconductor devices.[9]

The Hamiltonian of the DQDD is

$$H = H_D + H_E + H_{D-E} \ , \qquad (1)$$

where

$$H_D = \sum_{\ell=a,b} [U_\ell n_{\ell\uparrow} n_{\ell\downarrow} + \varepsilon_\ell (n_{\ell\uparrow} + n_{\ell\downarrow})] -$$
$$t_{ab} \sum_\sigma \left(d_{a\sigma}^\dagger d_{b\sigma} + d_{b\sigma}^\dagger d_{a\sigma} \right) . \qquad (2)$$
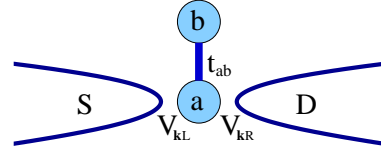

FIG. 1: Schematic representation of the device. A QD molecule with only one of the dots coupled to the leads.

describes the $a - b$ molecule and

$$H_E = \sum_{\mathbf{k},\sigma,\alpha} \varepsilon_\alpha(\mathbf{k}) \, c_{\mathbf{k}\sigma\alpha}^\dagger c_{\mathbf{k}\sigma\alpha} \ (\alpha = \mathrm{L,R}) \ , \qquad (3)$$

is the Hamiltonian of two non-interacting source and drain leads. The coupling between the molecule and the leads is described by the last term in the Hamiltonian,

$$H_{D-E} = \sum_{\mathbf{k},\sigma,\alpha} V_{\mathbf{k}\alpha} \left(d_{a\sigma}^\dagger \, c_{\mathbf{k}\sigma\alpha} + c_{\mathbf{k}\sigma\alpha}^\dagger \, d_{a\sigma} \right) . \qquad (4)$$

For symmetric leads, the conductance through the system is[12]

$$G(T) = \frac{e^2}{h} \Delta \pi \sum_\sigma \int_{-\infty}^\infty d\omega \left(-\frac{\partial f(\omega)}{\partial \omega} \right) \rho_{aa}^\sigma(\omega), \qquad (5)$$

where $\rho_{aa}^\sigma(\omega)$ is the local electronic density of states on dot a. Here, $\Delta = 2\pi\rho_0 \langle V_{\mathbf{k}}^2 \rangle$ where ρ_0 is the electronic density of states of the electrodes at the Fermi level, the brackets denote the average over the Fermi surface, and $f(\omega)$ is the Fermi function.

We solved the above model using the numerical renormalization group technique as well as an approximate analytical method that reproduces the main features of the numerical solution. Some exact results, that follow from the application of Luttinger's theorem to this system, are also given.

Our main findings are the following. The coupling t_{ab} is a relevant perturbation and the low-energy physics of the DQDD is fundamentally different from that of a single QD device. The zero-temperature conductance of the

system vanishes when the total charge of the device is an even integer and it is perfect when the charge is an odd integer. This is an exact result.

When both dots are nearly half-filled there are two different regimes for the temperature-dependence of the conductance depending on whether t_{ab} is small or large in a sense that will be made precise below. For small t_{ab}, a two-stage analog of the Kondo effect takes place with decreasing temperature. In the first stage, the magnetic moment of dot a is quenched by the electrons of the leads below some temperature. In the second stage, that occurs at a much lower temperature, the magnetic moment of dot b is in turn quenched by electrons that lie within the narrow Kondo resonance around the Fermi level. The two-stage Kondo effect results in a non-monotonic behavior of the conductance as a function of both gate voltage and magnetic field. In the regime of large t_{ab}, the magnetic moments of the dots form a tightly bound singlet weakly coupled to the leads and the conductance varies monotonically at low temperature.

When the charge on the device is varied by application of a gate voltage V_g, the zero-temperature conductance remains small in an extended interval of values of V_g. Conversely, in general, nearly perfect conductance is only observed in a very restricted range of values of the gate voltage.

A surprisingly rich variety of possibilities exists for the dependence of the conductance upon gate voltage and temperature depending upon the various parameters of the model.

The rest of the paper is organized as follows. In Section I we derive exact results for the dependence of the zero-temperature conductance of DQDD upon its charge and magnetization. The solution of the model within slave-boson mean-field theory is presented in Section II. Section III contains the description of our numerical results. Finally, we summarize our conclusions in Section V.

I. EXACT RESULTS

In the configuration depicted in Fig. 1 the ground state of a DQDD is expected to be a Fermi liquid. In this case, many exact results for the zero-temperature conductance of the device can be obtained using a simple generalization of Luttinger's theorem that we derive in the following.

Since electron-electron interactions do not involve the electronic states of the leads, the latter may be integrated out from the start. All the properties of the DQDD can then be expressed in terms of the reduced 2×2 retarded Green-function matrix

$$\mathbf{G}^{-1}(\omega) = \mathbf{G}_0^{-1}(\omega) - \mathbf{\Sigma}(\omega) , \qquad (6)$$

where $\mathbf{G}_0(\omega)$ is the non-interacting Green function,

$$\mathbf{G}_0^{-1}(\omega) = \begin{pmatrix} \omega - \epsilon_a + i\Delta & t_{ab} \\ t_{ab} & \omega - \epsilon_b \end{pmatrix} , \qquad (7)$$

and $\mathbf{\Sigma}(\omega)$ is the self-energy matrix.

The total number of electrons with spin σ in the dots at $T = 0$ is given by

$$n^\sigma \equiv n_a^\sigma + n_b^\sigma = -\frac{1}{\pi} \int_{-\infty}^0 d\omega \, \mathrm{Im} \left[\mathrm{Tr}\mathbf{G}(\omega) \right] , \qquad (8)$$

an expression that can be rewritten in the form

$$\begin{aligned} n_\sigma &= -\frac{1}{\pi} \, \mathrm{Im} \int_{-\infty}^0 d\omega \, \frac{\partial}{\partial\omega} \mathrm{Tr} \ln \mathbf{G}^{-1}(\omega) \\ &\quad - \frac{1}{\pi} \, \mathrm{Im} \int_{-\infty}^0 d\omega \, \mathrm{Tr} \left[\mathbf{G}(\omega) \frac{\partial}{\partial\omega} \mathbf{\Sigma}(\omega) \right] , \end{aligned} \qquad (9)$$

using the equality

$$\mathrm{Tr}\mathbf{G}(\omega) = \frac{\partial}{\partial\omega} \, \mathrm{Tr} \ln \mathbf{G}^{-1}(\omega) + \mathrm{Tr} \left[\mathbf{G}(\omega) \frac{\partial}{\partial\omega} \mathbf{\Sigma}(\omega) \right] , \qquad (10)$$

that can be easily checked using Eqs. (6) and (7).

The second integral on the right-hand side of Eq. (9) vanishes order by order in perturbation theory in $U_{a,b}$[13] which leads to

$$n_\sigma = \frac{1}{\pi} \left[\varphi(-\infty) - \varphi(0) \right] , \qquad (11)$$

where

$$\begin{aligned} \varphi(\omega) &= \mathrm{Im} \ln \Big\{ \left[\omega - \epsilon_a - \Sigma_{aa}(\omega) + i\Delta \right] \\ &\quad \times \left[\omega - \epsilon_b - \Sigma_{bb}(\omega) \right] - \left[t_{ab} - \Sigma_{ab}(\omega) \right]^2 \Big\} . \end{aligned} \qquad (12)$$

Introducing the renormalized parameters $\tilde{\epsilon}_a = \epsilon_a + \Sigma_{aa}(0)$, $\tilde{\epsilon}_b = \epsilon_b + \Sigma_{bb}(0)$, and $\tilde{t}_{ab} = t_{ab} - \Sigma_{ab}(0)$ we find:

$$n_\sigma = 2 - \frac{1}{\pi} \mathrm{Im} \ln \left[\tilde{\epsilon}_a \tilde{\epsilon}_b - \tilde{t}_{ab}^2 - i\Delta\tilde{\epsilon}_b \right] . \qquad (13)$$

For a Fermi-liquid ground state the self-energy matrix at the Fermi energy is purely real and so are the renormalized parameters. A straightforward calculation then yields:

$$n_\sigma = \frac{1}{\pi} \begin{cases} \delta , & \tilde{\epsilon}_a \text{ and } \tilde{\epsilon}_b > 0 , \ \tilde{\epsilon}_a \, \tilde{\epsilon}_b > \tilde{t}_{ab}^2 \\ 2\pi + \delta , & \tilde{\epsilon}_a \text{ and } \tilde{\epsilon}_b < 0 , \ \tilde{\epsilon}_a \, \tilde{\epsilon}_b > \tilde{t}_{ab}^2 \\ \pi + \delta , & \text{otherwise} \end{cases} \qquad (14)$$

where

$$\delta = \arctan \left(\frac{\tilde{\epsilon}_b \Delta}{\tilde{\epsilon}_a \tilde{\epsilon}_b - \tilde{t}_{ab}^2} \right) . \qquad (15)$$

In all cases we have the relationship

$$\left(\frac{\tilde{\epsilon}_b \Delta}{\tilde{\epsilon}_a \tilde{\epsilon}_b - \tilde{t}_{ab}^2} \right)^2 = \tan^2 \left(\pi n_\sigma \right) . \qquad (16)$$

Expressions (14)-(16) are identical to those that one would obtain for the non-interacting problem defined by Eq. (7) with the renormalized real parameters replacing the bare ones.

Similarly, the a-dot spectral density for spin σ at the Fermi energy is given by

$$\rho_{aa}^{\sigma}(0) = \frac{1}{\pi} \frac{\tilde{\epsilon}_b^2 \Delta}{\left(\tilde{\epsilon}_a \tilde{\epsilon}_b - \tilde{t}_{ab}^2\right)^2 + \left(\tilde{\epsilon}_b \Delta\right)^2} \, , \qquad (17)$$

which, using Eq. (16), can be cast in the form

$$\rho_{aa}^{\sigma}(0) = \frac{1}{\pi\Delta} \sin^2\left(\pi n_\sigma\right) \, . \qquad (18)$$

Equations (5) and (18) lead to the following expression for the conductance:

$$g \equiv \frac{G}{G_0} = \frac{1}{2} \sum_\sigma \sin^2\left[\pi\left(n_a^\sigma + n_b^\sigma\right)\right] \, , \qquad (19)$$

where $G_0 = 2e^2/h$ is the quantum of conductance.

In the absence of a magnetic field $n_\ell^\sigma = n_\ell^{-\sigma}$ and $g = \sin^2\left[\frac{\pi}{2}\left(n_a + n_b\right)\right]$ where $n_\ell = \sum_\sigma n_\ell^\sigma$. The zero-temperature conductance thus vanishes when the total number of electrons in the DQDD is even. This occurs in particular when $\varepsilon_\ell = -U_\ell/2$ for both dots. At this point the Hamiltonian is electron-hole symmetric and $n_a + n_b = 2$. Applying a gate voltage V_g that shifts the levels of the dots, the charge of the device varies continuously between $n_a + n_b = 0$ (for V_g large and negative) and $n_a + n_b = 4$ (for V_g large and positive). The conductance $g(V_g)$ vanishes at $V_g \to \pm\infty$ and $V_g = 0$ and has two maxima where it reaches the value $g = 1$ at the values of the gate voltage for which $n_a + n_b = 1$ or 3.

In the presence of a magnetic field B the dots polarize and a magnetization $m = \frac{1}{2}(n_\uparrow - n_\downarrow)$ appears. In the regime $n_a + n_b = 2$ Eq. (19) becomes

$$g = \sin^2(\pi m). \qquad (20)$$

In the low field limit g vanishes quadratically with B,

$$g \approx \pi^2 m^2 \approx \pi^2 B^2 \chi^2 = (B/B^\star)^2 \qquad (21)$$

were χ is the spin susceptibility and $B^\star = 1/(\pi\chi)$ defines a characteristic magnetic field. For very large B the dots become fully polarized, $m \to 1$, and the conductance also vanishes. At some intermediate field for which $m = 1/2$ the conductance has a maximum at which $g = 1$.

II. SLAVE BOSON MEAN FIELD THEORY

In this Section we present a mean-field slave-boson treatment[14,15,16] (SBMFT) of the problem. For simplicity we restrict ourselves to the electron-hole symmetric case in the most interesting regime in which the Coulomb repulsion on the dots $U_{a,b} \gg \Delta$. In this case the occupation of each dot is $n_\ell \sim 1$ and the low-energy excitations of the DQDD are spin fluctuations. These are described by the effective Hamiltonian

$$H_K = J_{ab}\mathbf{S}_a \cdot \mathbf{S}_b + J\mathbf{S}_a \cdot \mathbf{s}_0 + H_E. \qquad (22)$$

Here, $\mathbf{S}_\ell$ with $\ell = a, b$ are spin operators associated to the dots, and $\mathbf{s}_0 = \frac{1}{2}\sum_{s,s'} c_{0s}^\dagger \boldsymbol{\sigma}_{s,s'} c_{0s'}$ is the electron spin density on the orbital coupled to dot a. To leading order the coupling constant are $J_{ab} = 8t_{ab}^2/(U_a + U_b)$ and $J = 8\Delta/\pi U_a$.

Following standard methods[14,15,16] we represent the spin operators as $\mathbf{S}_\ell = \frac{1}{2}\sum_{s,s'} f_{\ell s}^\dagger \boldsymbol{\sigma}_{s,s'} f_{\ell s'}$ in terms of two pseudo-fermions constrained by the conditions $\sum_s f_{\ell s}^\dagger f_{\ell s} = 1$. The biquadratic interactions between the pseudo-fermions generated by the spin-spin interactions are decoupled introducing two Bose fields, B_a (conjugate to the amplitude $\sum_s f_{as}^\dagger c_{0s}$ and B_{ab} (conjugate to the amplitude $\sum_s f_{as}^\dagger f_{bs}$) and the constraints on occupations are implemented through Lagrange multipliers fields λ_ℓ. The free energy expressed in terms of the Bose fields has a saddle point at which the latter condense, $\langle B_a \rangle = \langle f_{a\sigma}^\dagger c_{0\sigma} \rangle$, $\langle B_{ab} \rangle = \langle f_{b\sigma}^\dagger f_{a\sigma} \rangle$, and the Lagrange multipliers vanish. The solution obtained by retaining only the saddle-point contribution to the free-energy is exact if the spin symmetry is extended from SU(2) to SU(N) and the limit $N \to \infty$ is taken. In the physical $N = 2$ case the SBMFT approach provides a simple and yet qualitatively accurate description of the low-energy properties of the system.

At the saddle point the effective Hamiltonian is

$$H_{\text{eff}} = \widetilde{J}_{ab}\sum_\sigma(f_{a\sigma}^\dagger f_{b\sigma}+h.c.)+\widetilde{J}\sum_\sigma(f_{a\sigma}^\dagger c_{0\sigma}+h.c.)+H_E, \qquad (23)$$

where the renormalized couplings are determined self-consistently by the equations

$$\frac{\pi\widetilde{J}_{ab}}{J_{ab}} = \int_{-D}^{D} d\omega \, f(\omega) \, \text{Im} \, \mathcal{G}_{ab}(\omega) \, , \qquad (24)$$

$$\frac{1}{J\rho_0} = -\int_{-D}^{D} d\omega \, f(\omega) \, \text{Re} \, \mathcal{G}_{aa}(\omega) \, , \qquad (25)$$

where

$$\mathcal{G}^{-1}(\omega) = \begin{pmatrix} \omega + i\widetilde{\Delta} & -\widetilde{J}_{ab} \\ -\widetilde{J}_{ab} & \omega \end{pmatrix} \, , \qquad (26)$$

and D is the half-width of the conduction band.

The system of equations (24)-(26) can be easily solved numerically. However, we shall focus below on some relevant limiting cases for which analytical expressions can be obtained.

A. Decoupled dots

For $J_{ab} = \widetilde{J}_{ab} = 0$ the model reduces to the well known Kondo Hamiltonian. The results for this model in the SBMFT approximation are well known.[16] In the weak-coupling limit $J\rho_0 \ll 1$ the solution of Eq. (25) at $T = 0$ is $\widetilde{\Delta}_0 = De^{-1/\rho_0 J}$. At finite temperatures solutions with non-zero $\widetilde{\Delta}_0$ only exist below a temperature $T_c = c_1 De^{-1/\rho_0 J}$, where c_1 is a constant of order

1. This approximation thus gives a spurious transition at which the spins and the conduction electrons decouple. In the exact solution of the Kondo model this sharp transition is replaced by a crossover at the Kondo temperature $T_K^0 \propto D e^{-1/\rho_0 J}$. We thus identify T_c with T_K^0.

The quasiparticle density of states is

$$\rho_{aa}(\omega) = \frac{1}{\pi} \frac{\widetilde{\Delta}_0}{\omega^2 + \widetilde{\Delta}_0^2} , \qquad (27)$$

describing a resonance of width $\widetilde{\Delta}_0$ at the Fermi level. The presence of this resonance leads to perfect conductance, $g = 1$, at zero temperature. The dot's magnetic susceptibility is $\chi_{aa} \propto 1/\left(\pi\widetilde{\Delta}_0\right)$.

B. Weakly coupled dots

In the limit in which the coupling between the dots is weak, $J_{ab} \ll \widetilde{\Delta}_0$, the solutions of the equations at $T = 0$ to leading order in $\widetilde{J}_{ab}/\widetilde{\Delta}$ are

$$\widetilde{J}_{ab} \sim \widetilde{\Delta} \exp\left(-\frac{\pi\widetilde{\Delta}}{2J_{ab}}\right) \qquad (28)$$

$$\widetilde{\Delta} \sim \widetilde{\Delta}_0 \left[1 - 2\left(\frac{\widetilde{J}_{ab}}{\widetilde{\Delta}_0}\right)^2 \ln\left(\frac{\widetilde{\Delta}_0}{\widetilde{J}_{ab}}\right)\right]. \qquad (29)$$

While $\widetilde{\Delta} \approx \widetilde{\Delta}_0$ remains essentially unchanged in this regime, the effective coupling between the dots is strongly suppressed. With increasing temperature $\widetilde{J}_{ab}$ further decreases and vanishes at a temperature

$$T_0 = c_2 \widetilde{\Delta}_0 \exp(-\frac{\pi\widetilde{\Delta}_0}{J_{ab}}) \propto \frac{\widetilde{J}_{ab}^2}{\widetilde{\Delta}_0} , \qquad (30)$$

where $c_2 \sim 1$ depends weakly on the parameters. As above, this transition temperature should be interpreted as a crossover temperature below which the magnetic moment of the dot b is screened.

Note that $T_0 \ll T_K^0$ which suggests a two-stage screening process.[11] First, the magnetic moment of dot a is screened by the electrons of the leads below T_K^0. Then, at the much lower temperature T_0, the magnetic moment of dot b is screened by the heavy quasiparticles of the local Fermi liquid that forms on dot a for $T \ll T_K^0$. The form of T_0 supports this physical picture as it corresponds precisely to the expression of the Kondo temperature of a magnetic moment screened by electrons of a band of width $\sim \widetilde{\Delta}_0$ and density of states $1/(\pi\widetilde{\Delta}_0)$.

The quasiparticle densities of states of the dots are

$$\rho_{aa}(\omega) = \frac{1}{\pi} \frac{\omega^2 \widetilde{\Delta}}{\left(\omega^2 - \widetilde{J}_{ab}^2\right)^2 + \left(\omega\widetilde{\Delta}\right)^2} , \qquad (31)$$

$$\rho_{bb}(\omega) = \frac{1}{\pi} \frac{\widetilde{J}_{ab}\widetilde{\Delta}}{\left(\omega^2 - \widetilde{J}_{ab}^2\right)^2 + \left(\omega\widetilde{\Delta}\right)^2} , \qquad (32)$$

respectively.

The first of these equations determines the conductance through the device. In the temperature range $T_0 \ll T \ll T_K^0$, where $\widetilde{J}_{ab}$ is irrelevant, we recover the usual Kondo resonance

$$\rho_{aa}(\omega) \sim \frac{1}{\pi} \frac{\widetilde{\Delta}}{\omega^2 + \widetilde{\Delta}^2} . \qquad (33)$$

This leads to a large conductance $g \approx 1$.

For $T \ll T_0$ and $\omega \ll \widetilde{J}_{ab}$,

$$\rho_{aa}(\omega) \sim \frac{1}{\pi\widetilde{\Delta}_0} \frac{\omega^2}{\omega^2 + \left(\widetilde{J}_{ab}^2/\widetilde{\Delta}_0\right)^2} . \qquad (34)$$

Therefore, ρ_{aa} vanishes at the Fermi energy where it has a dip of width $\propto T_0$. This dip is the analog of the Kondo hole that appears in the conduction-electron density of states in the usual Kondo problem. An immediate consequence of the presence of this hole is that the zero-temperature conductance of the DQDD vanishes at $T = 0$.

In the same limit, the magnetic susceptibility of the DQDD is dominated by the contribution of dot b. We find

$$\chi \approx \chi_{bb} = \frac{\widetilde{J}_{ab}^2}{\pi\widetilde{\Delta}_0} \propto \frac{1}{T_0} . \qquad (35)$$

Therefore, the magnetic scale $B^\star$ defined in Eq. (21) is also determined by T_0.

C. Strongly coupled dots

For $J_{ab} > \widetilde{\Delta}_0$ there are no solutions of Eqs. (24) and (25) with non-vanishing $\widetilde{\Delta}$. The dots remain decoupled from the leads and $\widetilde{J}_{ab} = J_{ab}/2$. The ground state is a singlet and there is a energy gap $E_g = 2\widetilde{J}_{ab} = J_{ab}$ in the electronic spectrum. Note that the singlet-triplet gap that results from the SBMFT treatment is the exact result for a pair of isolated dots.

The decoupling of the dots from the leads is an artifact of SBMFT. Presumably, the fluctuation corrections neglected in this approach generate a weak coupling between the spin singlet and the leads but we have not checked this point explicitly.

III. NUMERICAL RESULTS

In this section we present the numerical solution of the DQDD model obtained using the numerical renormalization group method (NRG)[17,18,19] modified to improve the accuracy in the computation of the spectral density.[20] We choose the half-bandwidth of the conduction band D as the unit of energy and consider for simplicity the case of identical dots, $\varepsilon_a = \varepsilon_b \equiv \varepsilon$ and $U_a = U_b \equiv U$.

We shall first discuss the electron-hole symmetric case in order to make contact with the SBMFT results of the previous Section.

A. Kondo screening

Figure 2 shows the NRG results for the temperature dependence of square of the total magnetic moment of the DQDD in the electron-hole symmetric case for several values of t_{ab}. The other parameters are $U = 0.5$, $\varepsilon = -0.25$, and $\Delta = 0.035$.

The magnetic moment μ is defined through the relationship $\mu^2 = T\chi$ where χ is the contribution of the quantum dots to the total magnetic susceptibility of the system.[17] For a free $S=1/2$ spin, $\mu^2 = 1/4$.

The uppermost curve in Fig. 2 represents the case of decoupled dots, $t_{ab} = 0$. At high temperatures (but low compared to U) the spins of both dots are free. Then $\mu^2 \to 1/2$. At some temperature scale there is a drop in μ^2 due to the Kondo screening of dot a. We identify this temperature with the Kondo temperature T_K^0 (a more precise determination of T_K^0 will be given in the following Section). Since the spin on dot b remains free down to $T = 0$, $\mu^2 = 1/4$ for $T \ll T_K^0$.

For any finite t_{ab} the total magnetic moment in the ground state vanishes and $\mu^2 \to 0$ as $T \to 0$. All the curves but the lowermost correspond to values of t_{ab} such that $J_{ab} \leq T_K^0$. It can be seen that, within this range of parameters, screening takes place in two stages as predicted by SBMFT. With decreasing temperature there is a first drop in μ^2 at the scale T_K^0 followed by a plateau. A second drop occurs at a much lower scale that we shall identify below with T_0. The temperature at which the first drop occurs is rather insensitive to the value of J_{ab} in agreement with Eq. (29). Note that the magnetic moment varies logarithmically with temperature at the two steps which confirms the two stages of screening are of the Kondo type as stated in the previous Section.

When t_{ab} increases the steps become closer, which signals a merging of the two scales with increasing J_{ab}, in agreement with Eq. (30).

We found that, in this low-J_{ab} regime and at low temperature, all the curves collapse onto a universal curve if the temperature is scaled by an appropriate factor T_{ab} that depends on J_{ab}. We expect on physical grounds $T_{ab} \propto T_0$. In order to check this hypothesis we calculated T_{ab} from the susceptibility data using the criterion $\mu^2(T_{ab}) = 1/8$. The results are represented with solid circles in the inset to Fig. 2. It is seen that T_{ab} varies exponentially with t_{ab}^{-2} in agreement with Eq. (30). The solid line is a fit to the SBMFT expression for T_0. An arbitrary multiplicative constant in the definition of T_{ab} was absorbed in c_2 and the parameter c_1 is the proportionality factor between T_K^0 and $\widetilde{\Delta}_0$. As expected, the values of c_1 and c_2 determined by the fit are $\mathcal{O}(1)$.

The lowermost curve shown in Fig. 2 corresponds to the case $J_{ab} > T_K^0$. It is seen that it is qualitative differ-
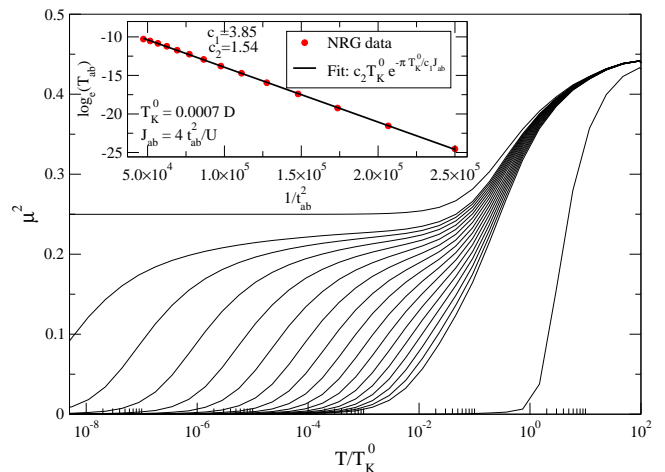

FIG. 2: Magnetic moment of the DQDD as a function of the temperature for different values of the interdot coupling. From top to bottom, $t_{ab} = 0$, $t_{ab} = 0.002 - 0.0046$ in steps of 0.0002, and $t_{ab} = 0.02$. Parameters are $U = 0.5$, $\varepsilon = -0.25$ and $\Delta = 0.035$. Inset: binding energy of the $a - b$ singlet T_{ab} estimated using the NRG (see text). The solid line is a fit based on Eq. (30).

ent from the others. In this regime the spins of the dots form a robust singlet weakly coupled to the leads. The susceptibility and the magnetic moment decrease exponentially in J_{ab}/T.

B. Spectral properties and conductance

Figure 3 shows the spectral density on dot a at zero temperature in the symmetric case for $U = 0.5$, $\Delta = 0.035$ and $t_{ab} = 0.0022$. This value corresponds to the third curve from the top in Fig. 2.

We observe three features, a very narrow central peak and two broad Coulomb peaks located at $\omega = \pm U/2$. We determine the Kondo scale $T_K^0 = 7 \times 10^{-4}$ from the full width at half-maximum of the central feature. The insets to the figure are zooms of the central peak. The left inset shows the Kondo peak plotted as a function of the reduced frequency ω/T_K^0. The right inset shows the Kondo hole in the density of states present over the tiny frequency interval $|\omega| < T_0 = 1.78 \times 10^{-10}$. This feature is obviously not visible on the scales of either the main plot or the left inset.

The conductance of the DQDD is entirely determined by the spectral density of dot a [cf. Eq. (5)]. The temperature dependence of g in zero magnetic field is represented in the lower panel of Fig. 4 for $t_{ab} = 3 \times 10^{-3}$ with the rest of the parameters fixed at the values given above. For temperatures $T > T_K^0$ the device is in the Coulomb blockade regime and the conductance is low. With decreasing temperature the Kondo correlations start to build up and the magnetic moment of dot a decreases as shown in the upper panel of the figure. For $T \lesssim T_K^0$
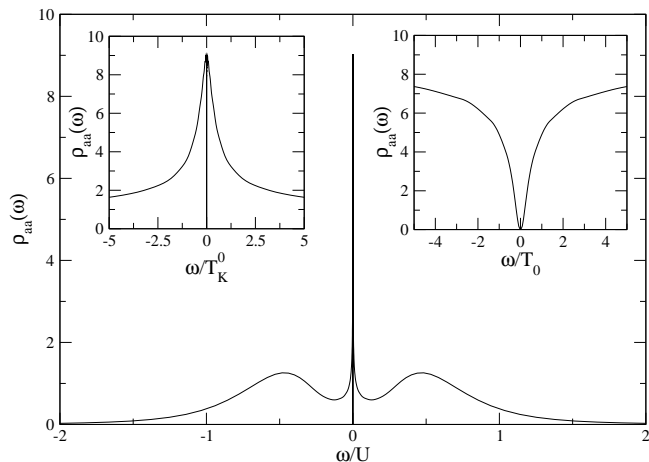
FIG. 3: Spectral density of dot a at $T = 0$. Parameters are $U = 0.5$, $\Delta = 0.035$ and $t_{ab} = 0.0022$. The broadened atomic levels of dot a are clearly seen at $\omega = \pm U/2$. The left inset shows the central Kondo peak of width $T_K^0 \sim 7 \times 10^{-4}$. The right inset shows the Kondo hole of width $T_0 \sim 1.78 \times 10^{-10}$.
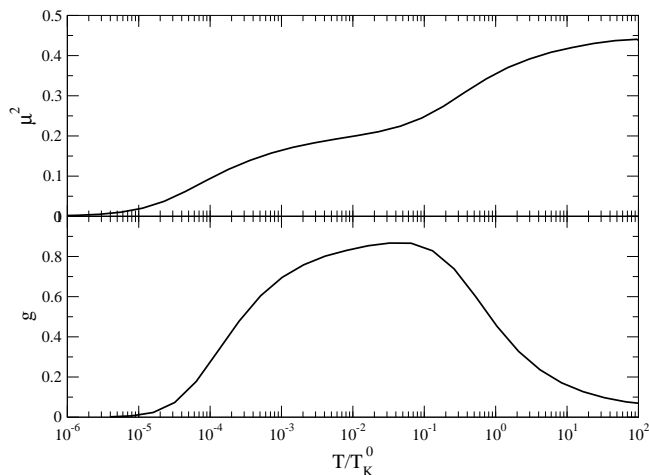

FIG. 4: Upper panel: Magnetic moment of the DQDD at zero field as a function of temperature for $t_{ab} = 0.003$. The other parameters are as in Fig.2. Lower panel: Conductance through the device at zero field as a function of the temperature. Three regimes can be clearly seen both in the conductance and the magnetic moment.

the spin on dot a is quenched resulting in resonant scattering through dot a and an enhanced conductance. For temperatures $T \lesssim T_0 \sim 7 \times 10^{-8}$, however, the spin of the second dot becomes also screened and the Kondo hole appears in the density of states. In this regime the conductance decreases again.

We now turn to a description of our results in the presence of a magnetic field. Data are displayed in Fig. 5 for the same parameters as in Fig. 4. The upper panel shows the field-dependence of the square of z-component of the total spin $\mathbf{S} = \mathbf{S_a} + \mathbf{S_b}$ of the DQDD at $T = 0$. The lower panel shows that of the conductance.

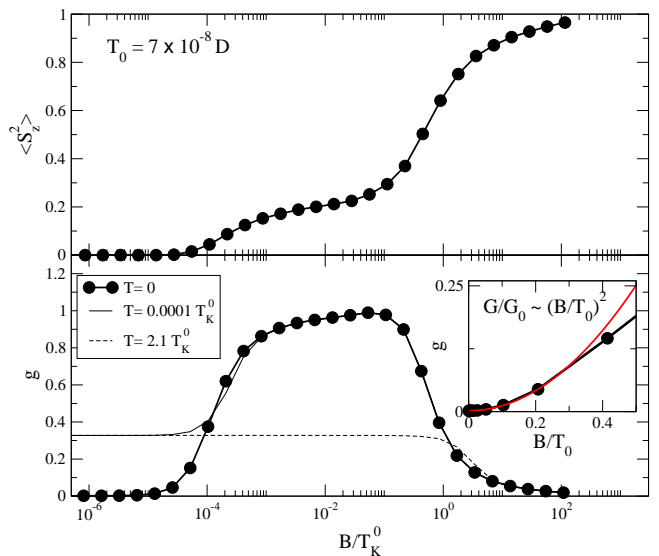For fields $B \gg T_K^0$ the spins of both dots are fully

FIG. 5: Upper panel : magnetic moment of the DQDD as a function of magnetic field at $T = 0$. Lower panel: conductance as a function of the magnetic field at low temperatures. Inset: Field-dependence of the $T = 0$ conductance. The coupling between the dots $t_{ab} = 0.003$. The other parameters are as in Fig.2.

polarized and $\langle S_z^2 \rangle = 1$. The Kondo effect can not take place and the conductance is small.

For $B < T_K^0$ the first stage of the Kondo effect takes place and the spin on dot a is quenched. At this point $\langle S_z^2 \rangle \sim 1/4$ indicating that the spin on dot b still remains polarized by the field. In this region of fields the conductance increases with decreasing field, approaching its maximum value, $g = 1$.

Upon further decrease of the field, Kondo screening of the second spin starts and, for $B \lesssim T_0 \approx 10^{-4} \times T_K^0$, it is in turn fully quenched. Then, the conductance decreases again and vanishes as $B \to 0$.

The inset to the figure shows that the low-field conductance varies quadratically with B with a characteristic field $B^\star \sim T_0$ in full agreement with Eqs. (21) and (35).

The effect of the temperature on the field-dependence of the conductance is also shown in the figure. For $T = 10^{-4}\ T_K^0 \approx T_0$ and fields $B > T$ the results are very similar to those obtained at zero temperature. At lower fields, however, the conductance saturates. This behavior arises because, at this temperature $T \gtrsim T_0$, quenching of spin b is only partial and the Kondo hole in the density of states ceases to develop. For $T > T_K^0$ both stages of the Kondo effect are suppressed by thermal fluctuations and the conductance is featureless as a function of B.

IV. CONDUCTANCE AS A FUNCTION OF THE GATE VOLTAGE

In this Section we discuss the dependence of the conductance upon the gate voltage. For simplicity we re-

strict the analysis to the case of identical dots $\varepsilon_a = \varepsilon_b = \varepsilon$, $U_a = U_b = U$. We have checked, however, that the results for other situations are qualitatively similar.

We display in Fig. 6 the conductance as function of ε, calculated from Eq. (5), for the set of parameters $U = 0.25, t_{ab} = 0.025$ and $\Delta = 0.125$. In this case the Kondo temperature and the effective magnetic coupling between the dots are $T_K^0 \sim \Delta$ and $J_{ab} \approx 0.01 < T_K^0$ for $\varepsilon = -U/2$.

At $T = 0$ we observe two peaks of perfect conductance, $g = 1$, and a wide region of low conductance between the two. The conductance vanishes at $\varepsilon = -U/2$ as discussed in the previous Section.

We have checked that the conductance at $T = 0$ satisfies Luttinger's theorem by computing g from Eq. (19) using the charge of the DQDD obtained from the NRG calculation and comparing it with the outcome of the direct calculation. The two results are the same within the numerical uncertainty.

The peaks of perfect conductance $g = 1$ occur when the DQDD is in either of the charge states $n_a + n_b = 1$ or $n_a + n_b = 3$. At large ε the charge of the DQDD is very small and increases with decreasing ε. It reaches $n = 1$ near $\varepsilon^\star$ such that the lowest energy level of the $a - b$ "molecule" crosses the Fermi level. In the absence of interactions this is $\varepsilon^\star = t_{ab}$. Interaction effects will reduce $\varepsilon^\star$, an effect that is already present for weak interactions for which a simple Hartree-Fock aproximation leads to $\varepsilon^\star = \sqrt{t_{ab}^2 + (U\delta/4)^2} - U/4$, where $\delta = n_b - n_a$ is the difference between the charges on the two dots. For our paramenters the reduction is very large and we find $\varepsilon^\star \approx 0.001 \ll t_{ab}$.

For temperatures $0 < T < T_K^0$, the conductance increases at the center of the valley due to the disappearance of the second stage of the Kondo efect. This leads to the three peak structure observed in the second and third panels from the bottom. If the temperature is further increased, the height of the conductance peaks decreases and, for temperatures $T \sim \Delta$, there is a single broad conductance peak. For our values of the parameters there are no Coulomb blockade peaks because their width Δ is comparable with their separation U.

Figure 7 shows the function $g(\varepsilon)$ at several temperatures for a different set of parameters, $U_a = U_b = 0.5$, $t_{ab} = 0.05$, and $\Delta = 0.063$. In this case, $T_K^0 \sim 0.01$ and $J_{ab} \sim 0.02 > T_K^0$. This a case in which the physics at the symmetric point is dominated by the formation of a strongly bound singlet between the spins of the two dots. The behavior at zero temperature is qualitatively similar to that found in the previous case. The evolution of the conductance with temperature is however quite different on two accounts. First, the conductance at $\varepsilon = -U/2$ is always a minimum; second, two additional conductance peaks appear upon rasing the temperature in the region $0 < T < T_K^0$. This phenomenon can be understood by noticing that while both J_{ab} and T_K^0 increase with ε in the valley away from $\varepsilon = -U/2$, the increase of T_K^0 is more pronounced because, in this case, the dependence on ε appears in the exponential. As result, while
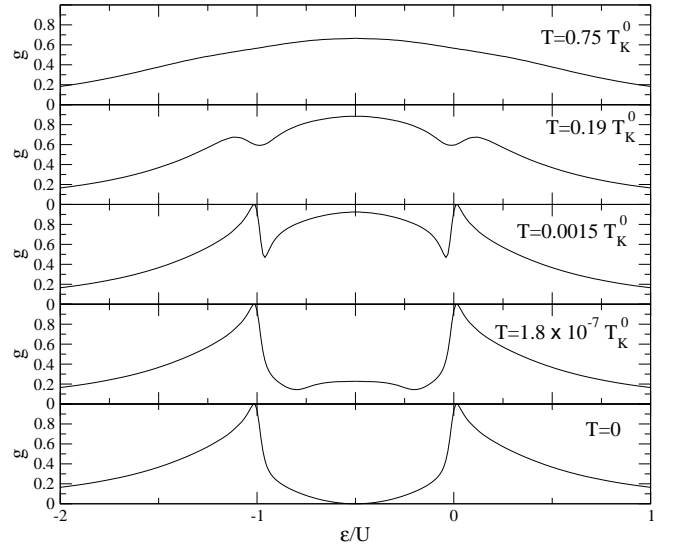

FIG. 6: Conductance through the double dot system as a function of the gate voltage $V_g = -\varepsilon_a = -\varepsilon_b = -\varepsilon$ and different temperatures. Parameters are $U_a = U_b = 0.25$, $t_{ab} = 0.025$ and $\Delta = 0.125$.
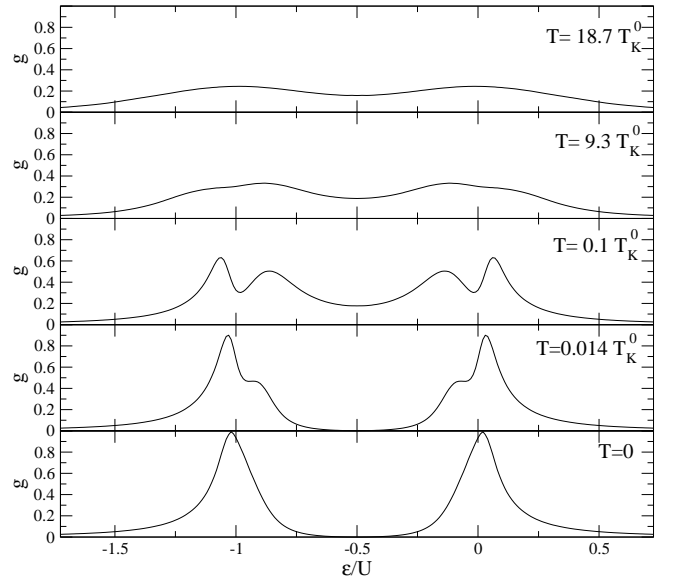

FIG. 7: Same as in Fig. 6 but for a different set of parameters: $U_a = U_b = 0.5$, $t_{ab} = 0.05$ and $\Delta = 0.063$.

$J_{ab} > T_K^0$ for $\epsilon = 0$ there is an inversion of the inequality for sufficiently large ϵ. When this inversion takes place the normal Kondo effect can occur and results in an enhancement of the conductance around some intermediate point. Finally, at high temperatures the usual Coulomb blockade peaks are this time visible because, for this parameter set, $\Delta \ll U$.

We close this Section with an analysis of a case in which the hopping matrix element between the dots is large. Fig. 8 shows results for $t_{ab} = 0.25 = U/2$ with all the other parameters as in Fig. 7. The appropriate
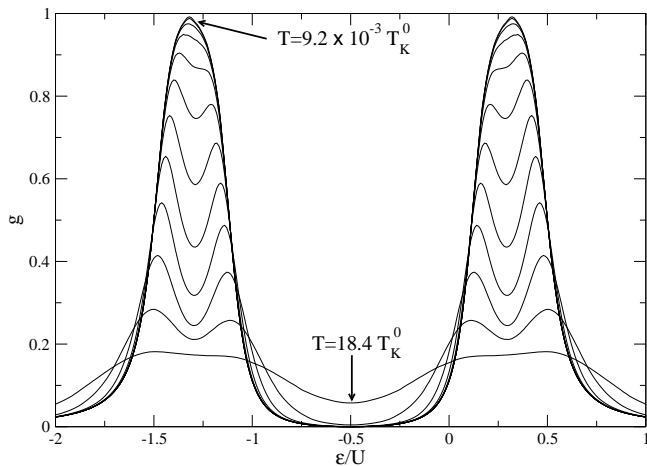
FIG. 8: Same as in Fig. 7 but for $t_{ab} = 0.25$. The curves correspond to temperatures ranging from $9.2 \times 10^{-3} T_K^0$ to $18.4 \ T_K^0$ from bottom to top (in the central region). Each curve corresponds to a temperature that is twice as high as that of the previous one.

starting point for a qualitative description of this case is an isolated $a - b$ molecule whose bonding and antibonding orbitals have energies $\varepsilon_{\pm} = \varepsilon \pm t_{ab}$. Consider the case in which the energy of the bonding orbital crosses the Fermi energy. The probability of occupation of the antibonding orbital is now strongly reduced because of the large energy gap $2t_{ab}$ that separates its energy from that of the bonding state. States with non-zero occupation of the antibonding state can then safely be projected out of the subspace of available states using a generalized Schrieffer-Wolff transformation just as one projects out states with double occupancy of either of the dots. The resulting effective problem describes a *single* quantum dot with renormalized parameters. We thus expect to observe the ordinary single-dot Kondo effect around $\varepsilon = t_{ab}$ and $\varepsilon = -t_{ab} - U$. This is precisely what the figure shows. At low T, there are two peaks of width $\sim U$ in the conductance in the range of values of ε for which the occupation number of the DDQD is odd. In the peak region we observe Coulomb blockade and the Kondo effect depending on the temperature. [29]

V. CONCLUSIONS

In summary, we studied the spectral, magnetic and transport properties of a double quantum-dot device in which one of the dots is coupled to perfect conducting leads.

The zero-temperature conductance of the system vanishes when the total charge of the device is an even integer and it is perfect when it is an odd integer.

When both dots are individually in the Kondo regime two different physical situations are possible depending on whether the magnetic coupling between the dots is

smaller or larger than the Kondo temperature of a single dot. When $J_{ab} \ll T_K^0$ the transport properties of the system reflect the existence of a two-stage Kondo effect. In the first one, the magnetic moment of the dot connected to the leads is screened at T_K^0, the Kondo temperature of the isolated dot. In this regime the conductance increases with decreasing temperature. At temperature $T_0 \ll T_K^0$ the magnetic moment of the second dot is also quenched, a process that leads to a conductance decreasing with temperature. A similar non-monotonic behavior is observed in the field-dependence of the conductance. In the opposite case, $J_{ab} \gg T_K^0$, the magnetic moments of the dots bind forming a strong singlet weakly coupled to the leads and the low temperature conductance decreases monotonically with T.

Application of a gate voltage leads to a rich variety of behaviors for the dependence of the conductance upon gate voltage and temperature. A general feature is that the conductance is small in a very wide range of values of V_g at all temperatures. At low temperatures, regions of nearly perfect conductance do exist, but they are restricted to narrow intervals of values of the gate voltage. Phenomena similar to some of those reported here have been found in a study of a multilevel quantum dot.[21]

In a recent paper[22] (see also Ref. 23) the same model was studied using exact diagonalization methods in small clusters. These authors investigate the zero-temperature conductance of the device as a function of the positions of the dot's energy levels $\varepsilon_{a,b}$. In the regime of small t_{ab} they report perfect conductance for $\varepsilon_a = \varepsilon_b = -U/2$. These numerical results are inconsistent with ours and, most importantly, with the implications of Luttinger's theorem. The exact diagonalization method apparently fails to capture the second stage of the Kondo effect responsible for the supression of the conductance at zero temperature.

The reason for this failure is easy to understand. In order to correctly describe the single dot Kondo effect in a finite cluster, the level spacing in the leads must be smaller than the Kondo temperature.[24,25,26,27,28] For a QD coupled to a linear chain the number of sites required is $N_s \gg 2D/T_K$ which becames numerically intractable beyond $N_s \sim 20$. Large Kondo temperatures must then be considered. The Kondo temperature of the second dot is much lower than T_K rending the problem intractable by the exact diagonalization method in the limit of small t_{ab}. However, these zero-temperature exact diagonalization results describe qualitatively the behavior for temperatures $T_0 < T \ll T_K^0$ or for large t_{ab}.

Finally, we want to stress that our conclusions are valid in the case in which the effective magnetic coupling between the dots J_{ab} is antiferromagnetic and do not apply directly to the case of ferromagnetic coupling.

VI. ACKNOWLEDGMENTS

[1] L. I. Glazman and M. E. Raikh, JETP Lett. **47**, 452 (1988).

[2] T. K. Ng and P. A. Lee, Phys. Rev. Lett. **61**, 1768 (1988).

[3] D. Goldhaber-Gordon, H. Shtrikman, D. Mahalu, D. Abusch-Magder, U. Meirav, and M. A. Kastner, Nature **391**, 156 (1998).

[4] A. Georges and Y. Meir, Phys. Rev. Lett. **82**, 3508 (1999).

[5] C. A. Büsser, E. V. Anda, A. L. Lima, M. A. Davidovich, and G. Chiappe, Phys. Rev. B **62**, 9907 (2000).

[6] J. C. Chen, A. M. Chang, and M. R. Melloch, Phys. Rev. Lett. **92**, 176801 (2004).

[7] W. G. van der Wiel, S. D. Franceschi, J. M. Elzerman, T. Fujisawa, S. Tarucha, and L. P. Kouwenhoven, Rev. Mod. Phys. **75**, 1 (2003).

[8] D. Loss and D. P. DiVincenzo, Phys. Rev. A **57**, 120 (1998).

[9] L. DiCarlo, H. J. Lynch, A. C. Johnson, L. I. Childress, K. Crockett, C. M. Marcus, M. P. Hanson, and A. C. Gossard, Phys. Rev. Lett. **92**, 226801 (2004).

[10] C. A. Büsser, A. Moreo, and E. Dagotto, Phys. Rev. B **70**, 035402 (2004).

[11] M. Vojta, R. Bulla, and W. Hofstetter, Phys. Rev. B **65**, 140405(R) (2002).

[12] Y. Meir and N. S. Wingreen, Phys. Rev. Lett. **68**, 2512 (1992).

[13] A. A. Abrikosov, L. P. Gorkov, and I. E. Dzyaloshinski, *Methods of Quantum Field Theory in Statistical Physics* (Prentice-Hall, Englewood-Cliffs, New Jersey, 1963).

[14] D. Newns and N. Read, Adv. Phys. **36**, 799 (1987).

[15] P. Coleman, Phys. Rev. B **35**, 5072 (1987).

[16] A. C. Hewson, *The Kondo Problem to Heavy Fermions* (Cambridge University Press, 1997).

[17] K. G. Wilson, Rev. Mod. Phys. **47**, 773 (1975).

[18] H. R. Krishna-murthy, J. W. Wilkins, and K. G. Wilson, Phys. Rev. B **21**, 1003 (1980).

[19] T. A. Costi, A. C. Hewson, and V. Zlatić, J. Phys.:Condens. Matter **6**, 2519 (1994).

[20] W. Hofstetter, Phys. Rev. Lett. **85**, 1508 (2000).

[21] W. Hofstetter and H. Schoeller, Phys. Rev. Lett. **88**, 016803 (2002).

[22] V. M. Apel, M. A. Davidovich, E. V. Anda, G. Chiappe, and C. A. Büsser, cond-mat/0404691.

[23] C. A. Büsser, G. B. Martins, K. A. Al-Hassanieh, A. Moreo, and E. Dagotto (2004), cond-mat/0404426.

[24] W. B. Thimm, J. Kroha, and J. von Delft, Phys. Rev. Lett. **82**, 2143 (1999).

[25] I. Affleck and P. Simon, Phys. Rev. Lett. **86**, 2854 (2001).

[26] P. S. Cornaglia and C. A. Balseiro, Phys. Rev. B **66**, 115303 (2002).

[27] P. Simon and I. Affleck, Phys. Rev. Lett. **89**, 206602 (2002).

[28] P. S. Cornaglia and C. A. Balseiro, Phys. Rev. Lett. **90**, 216801 (2003).

[29] We thank C. A. Büsser for pointing out to us that this effect was likely to occur.